Scheme I

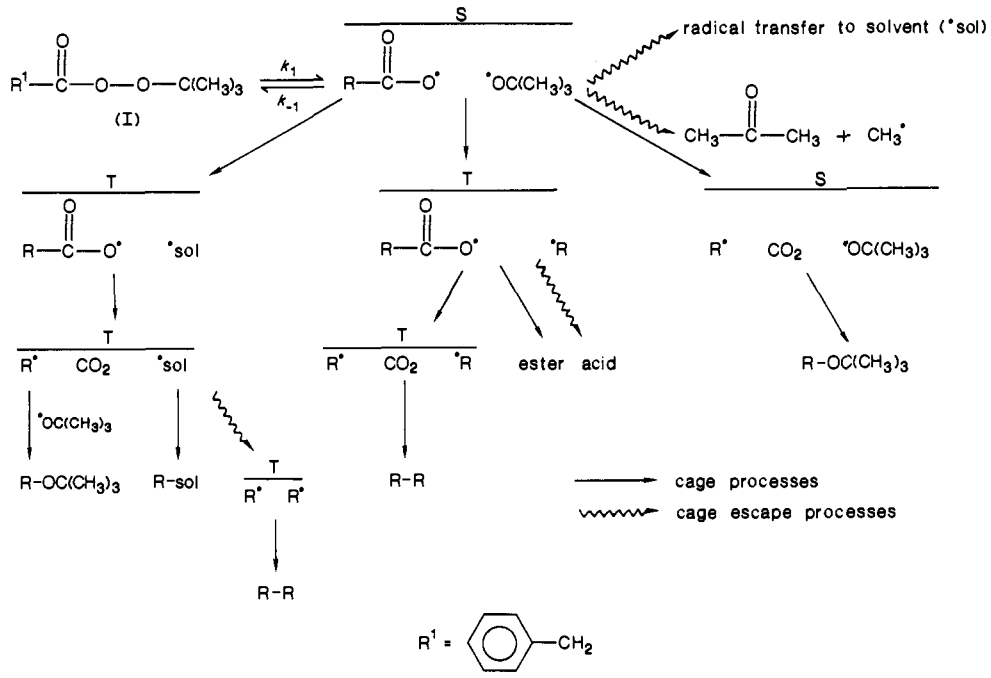

ies[11,17] and further supported by the C-13 CIDNP data. Since the *tert*-butyloxy radical cannot act as a radical pair partner, secondary triplet pairs form consisting of acyloxy–benzyl and acyloxy–solvent radical pairs. The acyloxy–benzyl triplet pair combine to a very small extent before decarboxylation. Evidence for this acyloxy intermediate in our CIDNP studies consists of the emissive polarizations of carbon dioxide and the C-13 labeled benzyl phenylacetate. The existence of the acyloxy radical as an intermediate has been corroborated by the recent work of Falvey and Schuster[19] and Lloyd and Williams.[20] The polarized bibenzyl arises from coupling after decarboxylation within the acyloxy–benzyl solvent cage or from escape from the acyloxy-solvent derived radial cage. The polarization observed for *cis*-stilbene is an example of a "memory effect",[18] with "spin sorting" occurring in the same step as in the bibenzyl case. Decarboxylation of the phenylacetyloxy radical in the initial singlet pair, with subsequent ether production, would not lead to polarization due to the inability of the *tert*-butoxy radical to act as a spin sorting partner. In hexachloroacetone the ether is formed in substantial amounts but shows no polarization, yet in cyclohexanone the C-2 and C-3 aromatic carbons show a strong enhanced absorption and emission, respectively. Knowing the signs of all other terms of the net equation, the phase of the polarizations indicate that the radical precursors leading to ether product had triplet multiplicity. The explanation for this is that in cyclohexanone the benzyl radical has a long enough lifetime that it attains concentrations high enough to scavenge *tert*-butoxy radicals which escape β-scission and reaction with solvent. This is an example of a scavenging process which is competitive with geminate recombination;[21] therefore, ether is produced by two pathways: within the primary cage which shows no polarization and in the bulk solution which leads to a polarized product. Evidence that solvent-derived radicals are involved in geminate pairs are the polarizations observed for benzyl chloride, benzyl pentachloroacetone, hexachloroethane, 1,1-dichlorostyrene,[22,23] toluene, and α-benzylcyclohexanone. Product studies also indicate that approximately 10% of the HCA is consumed during the decomposition.

Therefore, these CIDNP results indicate that *tert*-butyl phenylperacetate decomposes by a nonconcerted pathway with the observed rate of decomposition being dependent on the strength of the O–O bond, the rate of decarboxylation, and the rate of internal return.

(19) Falvey, D. E.; Schuster, G. B. *J. Am. Chem. Soc.* **1986**, *108*, 7419.
(20) Lloyd, R. V.; Williams, R. V. Presented at the Joint Southeast–Southwest ACS Regional Meeting, Memphis, TN, Oct. 9, 1985, unpublished results. ESR evidence of the acyloxy radical from *cis*- and *trans*-9-carbo-*tert*-butylperoxydecalin decomposition.
(21) Kaptein, R. *J. Am. Chem. Soc.* **1972**, *94*, 6262.
(22) The identification of polarizations of solvent-derived products was further conformed by their observation in all decompositions in HCA, NOE experiments during decomposition, and their observation during the thermal decomposition of di-*tert*-butyl peroxalate.
(23) den Hollander, J. A. *J. Chem. Soc., Chem. Comm.* **1975**, 352.

Vibrational Spectroscopic Characterization of the CCO Ligand and the Possible Occurrence of CCO on Surfaces

Michael J. Sailor and Duward F. Shriver*

Department of Chemistry, Northwestern University
Evanston, Illinois 60201
Received March 20, 1987

As outlined below there is abundant evidence from metal cluster chemistry that a carbon atom capping a three-metal array has a high affinity for CO, leading to the formation of CCO. Accordingly, we propose that CCO may exist on a carbided closest-packed metal surface in the presence of CO. For example, the surface carbide species on a Fischer–Tropsch catalyst[1-3] may be present as CCO. Vibrational spectroscopy represents one of the most promising methods for detecting CCO, and, therefore, we have undertaken vibrational characterization of CCO in the structurally characterized cluster $[Ru_3(CO)_6(\mu\text{-}CO)_3(\mu_3\text{-}CCO)]^{2-}$, **1**.

One striking example of the propensity of a capping C atom to couple with CO is the abstraction of halogen from a capping CX ligand to produce a capping CCO, eq 1.[4,5] Another example

(1) (a) Araki, M.; Ponec, V. *J. Catal.* **1976**, *44*, 439. (b) Kelley, R. D.; Goodman, D. W. *The Chemical Physics of Solid Surfaces and Heterogeneous Catalysis*; King, D. A., Woodruff, D. P., Ed.; Elsevier Scientific Publising Co: Amsterdam, 1982; p 445. (c) Dwyer, D. J.; Somorjai, G. A. *J. Catal.* **1978**, *52*, 291. (d) Kock, A. J. H. M.; Geus, J. W. *Prog. Surf. Sci.* **1985**, *20*, 165 and references contained therein.
(2) Biloen, P.; Helle, J. N.; Sachtler, W. M. H. *J. Catal.* **1979**, *58*, 95.
(3) Biloen, P.; Sachtler, W. M. H. *Adv. Catal.* **1981**, *30*, 165.
(4) Seyferth, D.; Williams, G. H.; Nivert, C. L. *Inorg. Chem.* **1977**, *16*, 758.

0002-7863/87/1509-5039$01.50/0

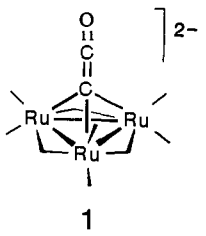

1

is the reductive cleavage of a capping COR, eq 2.[6,7] The conversion of a bridging CH_2 group to a capping CCO is also documented.[8,9] On the basis of this evidence for the stability and ease of formation of CCO in three-metal cluster compounds, we propose that carbide on a closest-packed metal surface may take on CO to form surface CCO.

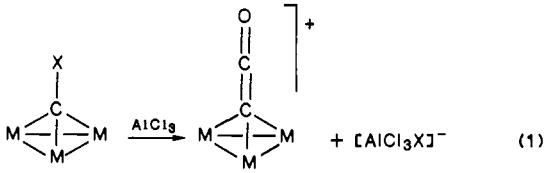

M = $Co(CO)_3$ or $HRu(CO)_3$

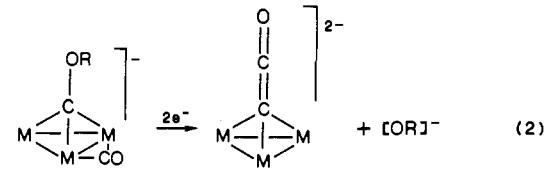

M = $Fe(CO)_3$, $Ru(CO)_3$, or $Os(CO)_3$

The cluster $[Ru_3(CO)_6(\mu\text{-}CO)_3(\mu_3\text{-}CCO)]^{2-}$, **1**, was chosen for study by IR and Raman spectroscopy because its X-ray structure approaches C_{3v} symmetry, and either or both of the CCO carbon atoms can be ^{13}C enriched.[10] Three normal modes of A_1 symmetry in the idealized C_{3v} point group are predicted for the CCO group attached to three metals. As it turns out, these are fairly well separated in frequency and can be described approximately as the M_3–C stretch, C–C stretch, and C–O stretch.

A prominent Raman band at 319 cm^{-1} is assigned to the M_3C stretch on the basis of its polarization ($\rho = 0.12$ in CH_2Cl_2 solution). The shift in this band upon isotopic substitution (CCO vs. $^{13}C^{13}CO$)[11] is barely discernable (ca. 4 cm^{-1}). The predicted shift based on a simple valence force field model is 7 cm^{-1}. The C–C stretch was not evident in survey IR and Raman spectra, but it was eventually identified as a weak polarized Raman band at 1309 cm^{-1}, that shifts by 32 cm^{-1} in the spectrum of solid $[PPN]_2[Ru_3(CO)_9(^{13}CCO)]$ (Figure 1). A shift of 25 cm^{-1} is calculated from a simple valence force field model for the Ru_3CCO moiety.

The CO stretch for the CCO ligand appears to be mixed with terminal CO stretches. For the combination of CCO and six terminal CO ligands there are three A_1 modes. Two of these can be identified as A_1 modes (2024 and 1980 cm^{-1}, Figure 2) by Raman depolarization ratios and the lack of splitting in the spectra of the solid, where the E modes are split by the low-site symmetry (C_1). Both the highest frequency band at 2024 cm^{-1} and the adjacent band at 1980 cm^{-1} shift in the $[Ru_3(CO)_6(\mu\text{-}CO)_3(\mu_3\text{-}^{13}C^{13}CO)]^{2-}$ isotopomer. Presumably coupling occurs between CCO and a metal-bound CO mode by a dipole–dipole mechanism.

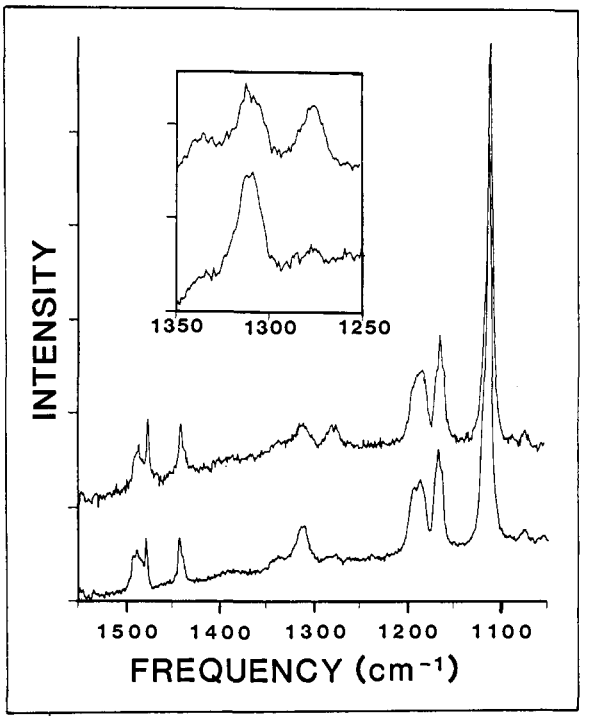

Figure 1. Raman spectrum of solid $[PPN]_2[Ru_3(CO)_6(\mu\text{-}CO)_3(\mu_3\text{-}CCO)]$, **1**, the lower trace at natural isotopic abundance and the upper trace at ca. 50% (μ_3-^{13}CCO). The inset shows an expanded view of the band assigned to ν_{cc} (lower trace is μ_3-CCO, upper is μ_3-*CCO, ca. 50% ^{13}C).

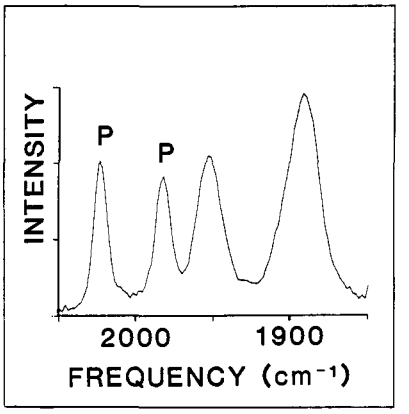

Figure 2. Raman spectrum in the terminal CO stretching region for a solution of $[PPN]_2[Ru_3(CO)_6(\mu\text{-}CO)_3(\mu_3\text{-}CCO)]$, **1**, in CH_2Cl_2. The bands marked with a P are polarized.

The vibrational frequencies for the CO ligand on a triruthenium cluster framework should be similar to those of a CCO moiety in a threefold site on a closest-packed metal surface, because the force field acting on the CCO is expected to be similar. Because the vibrational modes reported here for **1** involve CCO motions normal to the face of the metal triangle, they will belong to a set of vibrations that are favored by the "surface selection rule" for adsorbates on metal surfaces.[12] To our knowledge, surface bound CCO has not yet been observed. Infrared studies of CO on carbided Ni and Co surfaces have been performed,[13] and the EELS spectrum of H_2CCO on Fe has been recorded.[14] The presence of CCO on these surfaces was not considered. The most diagnostic

(5) Keister, J. B.; Horling, T. L. *Inorg. Chem.* **1980**, *19*, 2304.
(6) Kolis, J. W.; Holt, E. M.; Shriver, D. F. *J. Am. Chem. Soc.* **1983**, *105*, 7307.
(7) Sailor, M. J.; Shriver, D. F. *Organometallics* **1985**, *4*, 1476.
(8) Holmgren, J. S.; Shapley, J. R. *Organometallics* **1984**, *3*, 1322.
(9) Shapley, J. R.; Strickland, D. S.; St. George, G. M.; Churchill, M. R.; Bueno, C. *Organometallics* **1983**, *2*, 185.
(10) Sailor, M. J.; Brock, C. P.; Shriver, D. F. *J. Am. Chem. Soc.*, in press.
(11) The extent of ^{13}C enrichment of each isotopomer, made as described in ref 10, was checked by ^{13}C NMR of CD_2Cl_2 solutions of the samples. $[Ru_3(CO)_6(\mu\text{-}CO)_3(\mu_3\text{-}^*CCO)]^{2-}$ was ca. 50% enriched with ^{13}C at the starred position. Residual ^{13}C in all other CO carbons was <5%. The sample of $[Ru_3(CO)_6(\mu\text{-}CO)_3(\mu_3\text{-}^*C^*CO)]^{2-}$ was ca. 80% ^{13}C at the α-carbon (CCO) and 50% ^{13}C at the β-carbon atom (CCO). Residual ^{13}C on the metal bound carbonyls was determined to be <3%.
(12) Ibach, H.; Mills, D. L. *Electron Energy Loss Spectroscopy and Surface Vibrations*; Academic Press: New York, 1982; p 171.
(13) Moon, S. H.; Onuferko, J. H.; Window, H.; Katzer, J. R. *J. Vac. Sci. Technol.* **1981**, *18*, 467.
(14) McBreen, P. H.; Erley, W.; Ibach, H. *Surf. Sci.* **1984**, *148*, 292.

frequency for the detection of CCO, the C-C stretch, is weak in the infrared spectrum of clusters, so electron energy loss spectroscopy is a more promising technique than infrared for the detection of CCO on metal surfaces.

Acknowledgment. This research was supported by the Department of Energy Sciences Program, Grant no. DE-FG02-86ER13640.

Molecular Dynamics of the Primary Photochemical Event in Bacteriorhodopsin. Theoretical Evidence for an Excited Singlet State Assignment for the J Intermediate

Robert R. Birge,* Leonore A. Findsen, and Brian M. Pierce

Department of Chemistry, Carnegie Mellon University Pittsburgh, Pennsylvania 15213

Received March 23, 1987

The nature of the primary photochemical event in light-adapted bacteriorhodopsin (bR) has been studied by a variety of experimental[1-10] and theoretical[11] techniques. The picosecond time resolved absorption studies[5] are interpreted generally in terms of Scheme I. Raman,[6] FTIR,[7] NMR,[8] and optical[9] studies indicate

Scheme I

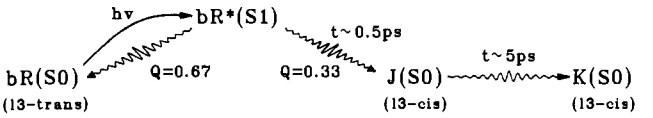

Scheme II

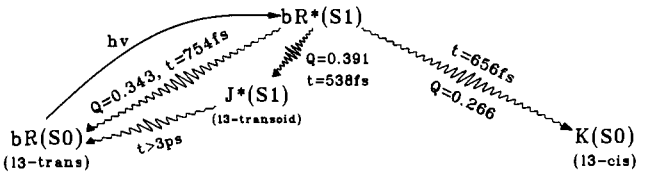

that K is an isomerized (13-cis) species. It is inferred that the chromophore in J is isomerized (13-cis) and that relaxation and/or proton translocation generates K.[2,3,5,11]

We studied the primary event in bacteriorhodopsin by using INDO-PSDCI SCF-MO theory and semiempirical molecular dynamics theory. Our procedures are identical with those used previously to study rhodopsin.[12-14] We generated our models of bR (Figure 1a) and K (Figure 1b) by using molecular orbital theory to predict bR and K absorption spectra and energy differences and optimizing the structures to best reproduce the experimental data.[9,10a] The calculated potential surfaces, Franck-Condon absorption maxima and photoisomerization dynamics associated with the absorption of light, are shown in Figure 1c-f. The shape of the lowest lying excited singlet state potential surface, however, is far from optimum for dynamic coupling into the ground state. The S_1 surface has a positive hump at the 270° ΔE_{10} minimum which reduces dramatically the coupling efficiency (see Discussion in ref 12 and 13). This characteristic of the S_1 surface was observed in all of our calculations, irrespective of model, and differs significantly from the corresponding feature calculated for the S_1 surface of rhodopsin.[11c-13] The rhodopsin S_1 surface has a relatively deep potential well at the ΔE_{10} surface minimum which traps the trajectory in an activated complex resulting in excellent dynamic coupling into the ground state.[12,13] This difference in potential surfaces results in a rhodopsin → bathorhodopsin quantum yield (0.62)[12] which is roughly twice that calculated for the bR → K phototransformation (0.27; see below).

Our calculations predict complex dynamics and biphasic repopulation of bR involving three pathways depopulating the S_1^* potential surface (Scheme II). Only one pathway leads to a vibrationally relaxed 13-cis ground-state species in 656 fs (λ_{max} = 621 nm, Q = quantum yield = 0.266). A second dynamic pathway regenerates vibrationally relaxed bR in 754 fs (λ_{max} = 559 nm, Q = 0.343). The third pathway populates a metastable 13-transoid excited singlet state species in 538 fs (λ_{max} = 650 nm, Q = 0.391). This population decays via nondynamic processes to reform bR exclusively (Figure 1e). We label this species "J" for reasons outlined below.

Calculated transient one-photon absorption spectra of the ensemble of excited species are shown in Figure 1g. These spectra were generated by using oscillator strength weighted Gaussian wavepacket propagation theory,[15] a basis set consisting of the 16 lowest lying excited singlet states and a 300 fs Gaussian excitation pulse. We assumed that the time constant for decay of the trapped S_1 species (Figure 1e) was 6 ps based on model compound studies.[9c] Individual components or component mixtures are responsible for

(1) For relevant Reviews see 2-4.
(2) Ottolenghi, M. *Adv. Photochem.* **1980**, *12*, 97-200.
(3) Birge, R. R. *Annu. Rev. Biophys. Bioeng.* **1981**, *10*, 315-54.
(4) Stoeckenius, W.; Bogomolni, R. *Annu. Rev. Biochem.* **1982**, *52*, 587-616.
(5) (a) Polland, H.-J.; Franz, M. A.; Zinth, W.; Kaiser, W.; Kölling, E.; Oesterhelt, D. *Biophys. J.* **1986**, *49*, 651-662. (b) Sharkov, A. V.; Pakulev, A. V.; Chekalin, S. V.; Matveetz, Y. A. *Biochim. Biophys. Acta* **1985**, *808*, 94-102. (c) Petrich, J. W.; Breton, J.; Martin, J. L. *Biophys. J.* **1987**, *51*, 416a. (d) Ippen, E. P.; Shank, C. V.; Lewis, A.; Marcus, M. A. *Science (Washington, DC)* **1978**, *200*, 1279-1281; Shichida, Y.; Matuoka, S.; Hidaka, Y.; Yoshizawa, T. *Biochim. Biophys. Acta* **1983**, *723*, 240-246. (e) Kaufmann, K. J.; Rentzepis, P. M.; Stoeckenius, W.; Lewis, A. *Biochem. Biophys. Res. Commun.* **1976**, *68*, 1109-1115; Kaufmann, K. J.; Sundstrom, V.; Yamane, T.; Rentzepis, P. M. *Biophys. J.* **1978**, *22*, 121-124. Applebury, M. L.; Peters, K. S.; Rentzepis, P. M. *Biophys. J.* **1978**, *23*, 375-382.
(6) Smith, S. O.; Lugtenburg, J.; Mathies, R. A. *J. Membr. Biol.* **1985**, *85*, 95-109. Smith, S. O.; Myers, A. B.; Pardoen, J. A.; Winkel, C.; Mulder, P. P. J.; Lugtenburg, J.; Mathies, R. *Proc. Natl. Acad. Sci. U.S.A.* **1984**, *81*, 2055-2059; Braiman, M.; Mathies, R. *Proc. Natl. Acad. Sci. U.S.A.* **1982**, *79*, 403-407; Aton, B.; Doukas, A. G.; Callender, R. H.; Becher, B.; Ebrey, T. G. *Biochemistry* **1977**, *16*, 2995-2999. Stockburger, M.; Klusmann, W.; Gattermann, H.; Massig, G.; Peters, R. *Biochemistry* **1979**, *18*, 4886-4900. Hsieh, C.-L.; Nagumo, M.; Nicol, M.; El-Sayed, M. A. *J. Phys. Chem.* **1981**, *85*, 2714-2717. Terner, J.; Hsieh, C.-L.; Burns, A. R.; El-Sayed, M. A. *Proc. Natl. Acad. Sci. U.S.A.* **1979**, *76*, 3046-3050.
(7) Rothschild, K. J.; Roepe, P.; Gillespie, J. *Biochim. Biophys. Acta* **1985**, *808*, 140-147. Bagley, K.; Dollinger, G.; Eisenstein, L.; Singh, A. K.; Zimanyi, L. *Proc. Natl. Acad. Sci. U.S.A.* **1982**, *79*, 4972-4976. Siebert, F.; Mäntele, F. *Eur. J. Biochem.* **1983**, *130*, 565-573.
(8) Harbison, G. S.; Smith, S. O.; Pardoen, J. A.; Courtin, J. M. L.; Lugtenburg, J.; Herzfeld, J.; Mathies, R. A.; Griffin, R. G. *Biochemistry* **1985**, *24*, 6955-6962.
(9) (a) Goldschmidt, C. R.; Ottolenghi, M.; Korenstein, R. *Biophys. J.* **1976**, *16*, 839-843. Hurley, J. B.; Ebrey, T. G. *Biophys. J.* **1978**, *22*, 49-66. Goldschmidt, C. R.; Kalisky, O.; Rosenfeld, T.; Ottolenghi, M. *Biophys. J.* **1977**, *17*, 179-183. (b) Oesterhelt, D.; Hess, B. *Eur. J. Biochem.* **1973**, *37*, 316-326. (c) Polland, H.-J.; Franz, M. A.; Zinth, W.; Kaiser, W.; Kölling, E.; Oesterhelt, D. *Biochim. Biophys. Acta* **1984**, *767*, 635-639. Fang, J.-M.; Carriker, J. D.; Balogh-Nair, V.; Nakanishi, K. *J. Am. Chem. Soc.* **1983**, *105*, 5162-5164. Kölling, E.; Gärtner, W.; Oesterhelt, D.; Ernst, L. *Angew. Chem. Int. Ed Engl.* **1984**, *23*, 81-82. (d) Kouyama, T.; Kinosita, K.; Ikegami, A. *Biophys. J.* **1985**, *47*, 43-54. Iwasa, T.; Tokunaga, F.; Yoshizawa, T. *Biophys. Struct. Mech.* **1980**, *6*, 253-270.
(10) (a) Birge, R. R.; Cooper, T. M. *Biophys. J.* **1983**, *42*, 61-69. (b) Ort, D. R.; Parson, W. W. *Biophys. J.* **1979**, *25*, 355-364.
(11) (a) Dinur, U.; Honig, B.; Ottolenghi, M. *Photochem. Photobiol.* **1981**, *33*, 523-527. (b) Schulten, K.; Tavan, P. *Halobacterium halobium. Nature (London)* **1978**, *272*, 85-86. Tavan, P.; Schulten, K. *Biophys. J.* **1986**, *50*, 81-89. (c) Birge, R. R.; Pierce, B. M. In *Photochemistry and Photobiology*; Zewail, A., Ed.; Hardwood Academic: New York, 1982; Vol. 2, pp 841-855.
(12) Birge, R. R.; Hubbard, L. M. *J. Am. Chem. Soc.* **1980**, *102*, 2195-2205. Birge, R. R.; Hubbard, L. M. *Biophys. J.* **1981**, *34*, 517-534.
(13) Birge, R. R. In *Biological Events Probed by Ultrafast Laser Spectroscopy*; Alfano, R. R., Ed.; Academic Press: New York, 1982; pp 299-317.
(14) The vibrational relaxation rate parameter ($|\Delta E_{vib}/\Delta t|_{avg}$) was set equal to 5 eV·ps^{-1} and the density of states factor (ρ) was set equal to 2 eV^{-1}. These parameters were adjusted upward (toward increased vibrational relaxation) until wavelength-independent quantum yields were observed (see ref 12 and 13). Test calculations indicate that the principal conclusions of this study are invariant to reasonable changes in parameterization.
(15) Tannor, D. J.; Heller, E. J. *J. Chem. Phys.* **1982**, *77*, 202-218. Birge, R. R.; Pierce, B. M. *Int. J. Quant. Chem.* **1986**, *29*, 639-656.

0002-7863/87/1509-5041$01.50/0